iScience

CellPress
OPEN ACCESS

Article

Niche-expressed Galectin-1 is involved in pre-B acute lymphoblastic leukemia relapse through pre-B cell receptor activation

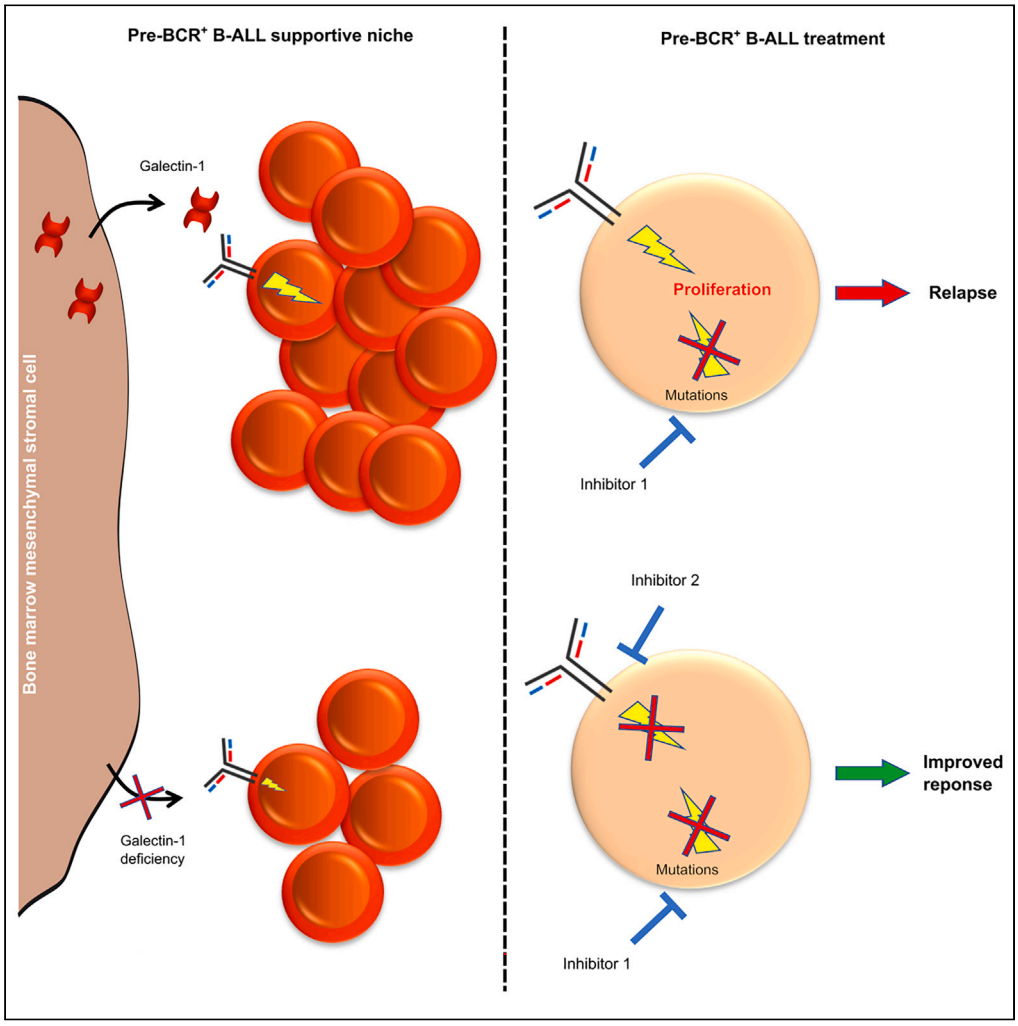

Jeoffrey Pelletier, Marielle Balzano, Jérôme Destin, ..., Norbert Vey, Michel Aurrand-Lions, Stéphane J.C. Mancini

stephane.mancini@univ-rennes.fr

Highlights

Galectin-1 produced by the bone marrow microenvironment influences pre-B ALL growth

Growth signals are transmitted to pre-B ALL through GAL1-dependent pre-BCR signaling

Targeting non-cell-autonomous cues can decrease resistance to common treatments

Pelletier et al., iScience *26*, 106385
April 21, 2023
https://doi.org/10.1016/j.isci.2023.106385

iScience

CellPress
OPEN ACCESS

Article

Niche-expressed Galectin-1 is involved in pre-B acute lymphoblastic leukemia relapse through pre-B cell receptor activation

Jeoffrey Pelletier,[1] Marielle Balzano,[1] Jérôme Destin,[2] Camille Montersino,[1] Marjorie C. Delahaye,[1] Tony Marchand,[2] Anne-Laure Bailly,[1] Florence Bardin,[1] Emilie Coppin,[1,7] Armelle Goubard,[1] Remy Castellano,[1] Marjolein J.W. de Bruijn,[3] Jasper Rip,[3,8] Yves Collette,[1] Patrice Dubreuil,[1] Karin Tarte,[2] Cyril Broccardo,[4] Rudi W. Hendriks,[3] Claudine Schiff,[5] Norbert Vey,[1,6] Michel Aurrand-Lions,[1] and Stéphane J.C. Mancini[1,2,9,*]

SUMMARY

B-cell acute lymphoblastic leukemia (B-ALL) reflects the malignant counterpart of developing B cells in the bone marrow (BM). Despite tremendous progress in B-ALL treatment, the overall survival of adults at diagnosis and patients at all ages after relapse remains poor. Galectin-1 (GAL1) expressed by BM supportive niches delivers proliferation signals to normal pre-B cells through interaction with the pre-B cell receptor (pre-BCR). Here, we asked whether GAL1 gives non-cell autonomous signals to pre-BCR$^+$ pre-B ALL, in addition to cell-autonomous signals linked to genetic alterations. In syngeneic and patient-derived xenograft (PDX) murine models, murine and human pre-B ALL development is influenced by GAL1 produced by BM niches through pre-BCR-dependent signals, similarly to normal pre-B cells. Furthermore, targeting pre-BCR signaling together with cell-autonomous oncogenic pathways in pre-B ALL PDX improved treatment response. Our results show that non-cell autonomous signals transmitted by BM niches represent promising targets to improve B-ALL patient survival.

INTRODUCTION

B-cell acute lymphoblastic leukemia (B-ALL) affects differentiating B cells in bone marrow (BM). B-ALLs are not only classified by their cytogenetic status, but also according to the subset in which the developmental arrest occurred, based on immunophenotyping.[1,2] The latest international consensus classification now also takes into consideration new subcategories of ALL based on distinctive gene signatures.[3] Pre-B ALL (BIII-ALL according to the European Group for Immunophenotypic characterization of Leukemias, EGIL) is the leukemic counterpart of pre-B cells expressing the pre-B cell receptor (pre-BCR). The pre-BCR is composed of the immunoglobulin μ heavy chain (IgH), the expression of which follows the successful rearrangement of IgH genes, associated with the surrogate light chain (SLC). Pre-BCR expression induces pre-B cell survival, proliferation, and differentiation.[4] Pre-B ALL express a functional pre-BCR that efficiently activates downstream signaling proteins, including SYK, BLNK, and BTK. Furthermore, pre-BCR signaling is sensitive to specific tyrosine kinase inhibitors such as the BTK inhibitor Ibrutinib,[5,6] suggesting that pre-BCR signaling is a potential therapeutic target in this pathology.

B-ALL with a t(1; 19) translocation, yielding an E2A::PBX1 fusion gene, represent the main sub-type among pre-BCR$^+$ pre-B ALL.[5] In addition, a small proportion of t(9; 22) patients expressing the BCR::ABL1 oncogenic fusion product - found in 3% and 25% of pediatric and adult B-ALL respectively[1] - were also classified as pre-BCR$^+$.[7] As a whole, It has been found in a cohort of 830 patients that 13.5% of the B-ALLs corresponded to pre-B ALL expressing a functional pre-BCR.[5] Genetic alterations including fusion gene products drive cell-autonomous signals, although it has become clear that cues from the BM microenvironment can also sustain B-ALL development and induce resistance to treatments and relapse.[8] The current knowledge on the involved mechanisms remains however limited. Although in non-malignant pre-B cells there is clear evidence for ligand-independent autonomous pre-BCR signaling,[9] binding of Galectin-1 (GAL1) - an s-type lectin expressed in particular by BM mesenchymal

[1]Aix Marseille University, CNRS, INSERM, Institut Paoli-Calmettes, CRCM, Marseille, France

[2]University Rennes, INSERM, EFS, UMR S1236, Rennes, France

[3]Department of Pulmonary Medicine, Erasmus MC, University Medical Center, Rotterdam, the Netherlands

[4]Centre de Recherche en Cancérologie de Toulouse, INSERM UMR-1037, Université de Toulouse III Paul Sabatier, Toulouse, France

[5]Aix Marseille University, CNRS, INSERM, CIML, Marseille, France

[6]Department of Hematology, Institut Paoli-Calmettes, Marseille, France

[7]Present address: Immunology of Aging, Leibniz Institute on Aging—Fritz Lipmann Institute, Jena, Germany

[8]Present address: Department of Immunology, Erasmus MC, University Medical Center, Rotterdam, The Netherlands

[9]Lead contact

*Correspondence: stephane.mancini@univ-rennes.fr

https://doi.org/10.1016/j.isci.2023.106385

stromal cells (MSC) - to the SLC was shown to trigger pre-BCR activation in normal pre-B cells.[10,11] Whether GAL1 present in the leukemic microenvironment participates to pre-B ALL pathogenesis through pre-BCR signaling remains unknown. Our current work demonstrates that GAL1 effectively sustains pre-B ALL development through pre-BCR activation, in addition to signals transmitted by driver mutations present in the leukemic cells.

RESULTS

GAL1 favors murine pre-BCR$^+$ B-ALL development

To investigate the influence of GAL1 on leukemic pre-B cells, we took advantage of *Blnk*$^{-/-}$*Btk*$^{-/-}$ mice which spontaneously develop pre-BCR$^+$ pre-B ALL.[12] Pre-B ALL isolated from these mice were injected intravenously into WT and the GAL1-deficient *Lgals1*$^{-/-}$ mice (Figures S1A and S1B). Interestingly, while 75% of WT mice died of leukemia within 13 days, most *Lgals1*$^{-/-}$ mice survived at least for 35 weeks and only 15.4% died within 21 days (Figure 1A). Accordingly, the proportion of leukemic cells in the BM 8 days after injection was significantly higher in WT than in *Lgals1*$^{-/-}$ mice (Figure 1B). This result was confirmed in another model of pre-BCR$^+$ leukemia developing spontaneously in mice expressing the PAX5-ELN fusion protein identified in human B-ALL[13] (Figures S1C and S1D). Importantly, the difference in tumor burden was not due to a decreased homing of *Blnk*$^{-/-}$*Btk*$^{-/-}$ leukemic cells to the BM, because similar numbers were found in the parenchyma of WT and *Lgals1*$^{-/-}$ mice 1 day after injection (Figures S1E and S1F). It has also been shown that GAL1 could induce T cell apoptosis and restrain T cell activation and expansion, leading to decreased tumor rejection.[14–16] One could therefore argue that the impaired development of pre-B ALL cells in absence of GAL1 may be linked to an increase in effector T cells in the BM. Early (d1) and late (d6) after leukemic cell homing into the BM, the proportions of both CD4$^+$ and CD8$^+$ total T cells, as well as effector CD44$^+$ T cells, were similar for WT and *Lgals1*$^{-/-}$ mice (Figures S1G). Furthermore, leukemic cell survival was similar in mice of both genotypes at d1 and d6 (Figure S1H), suggesting that the decreased leukemic load in *Lgals1*$^{-/-}$ mice was mostly due to a growth defect and not to an increased rejection by T cells.

Common B-ALL do not express the μ H chain and thus the pre-BCR. They are phenotypically close to pre-B ALL since they express the other components of the pre-BCR cascade.[17–19] Using common B-ALL obtained from Eμ-Myc mice (Figures S1A and S1B), we further assessed the expression of the α4β1, α5β1, and α4β7 integrins required for GAL1-dependent pre-BCR signaling[20] and found that they expressed similar levels as *Blnk*$^{-/-}$*Btk*$^{-/-}$ pre-B ALL (Figures S1I). Despite these phenotypic similarities with pre-B ALL, both survival curves and growth of common B-ALL obtained from Eμ-Myc mice, were comparable upon engraftment into WT and *Lgals1*$^{-/-}$ mice (Figures 1C and 1D). Taken together, these findings suggest that GAL1-induced B-ALL growth may depend on pre-BCR expression.

Finally, as GAL1 potentiates pre-BCR signaling,[20,21] the phosphorylation of SYK tyrosine kinase, activated early upon pre-BCR activation,[4] was analyzed following *Blnk*$^{-/-}$*Btk*$^{-/-}$ pre-B ALL injection. As expected, SYK phosphorylation in pre-B ALL cells was significantly decreased in the absence of GAL1 (Figure 1E). Altogether, these results strongly suggest that GAL1 favors murine pre-B ALL development through pre-BCR signaling.

GAL1 produced by the bone marrow microenvironment favors murine pre-BCR$^+$ B-ALL outgrowth

To determine the importance of GAL1 expressed by the non-hematopoietic BM microenvironment on pre-B ALL growth, stroma KO chimeric mice were obtained by transplanting WT donor BM to *Lgals1*$^{-/-}$ mice. WT recipients reconstituted with WT donor BM served as controls. Following injection of *Blnk*$^{-/-}$*Btk*$^{-/-}$ pre-B ALL cells, BM leukemic cells were significantly reduced in stroma KO mice compared to WT controls (Figure 2A). This result indicates that GAL1 expressed by non-hematopoietic cells of the BM plays an important role in pre-B ALL growth. *Blnk*$^{-/-}$*Btk*$^{-/-}$ Pre-B ALL were then co-cultured with MSCs derived from WT and *Lgals1*$^{-/-}$ mice that were phenotypically similar but distinct in terms of GAL1 expression (Figure S1J). As observed *in vivo*, pre-B ALL growth was more robust in the presence of GAL1 than in its absence and was correlated with an increased proliferation (Figures 2B and 2C). Furthermore, although not detected *in vivo* potentially because of a rapid elimination by macrophages, apoptotic cells were significantly increased in the absence of GAL1 (Figure 2C). Altogether, these results show that GAL1 expressed by BM MSCs is implicated in the expansion of murine pre-BCR$^+$ pre-B ALL.

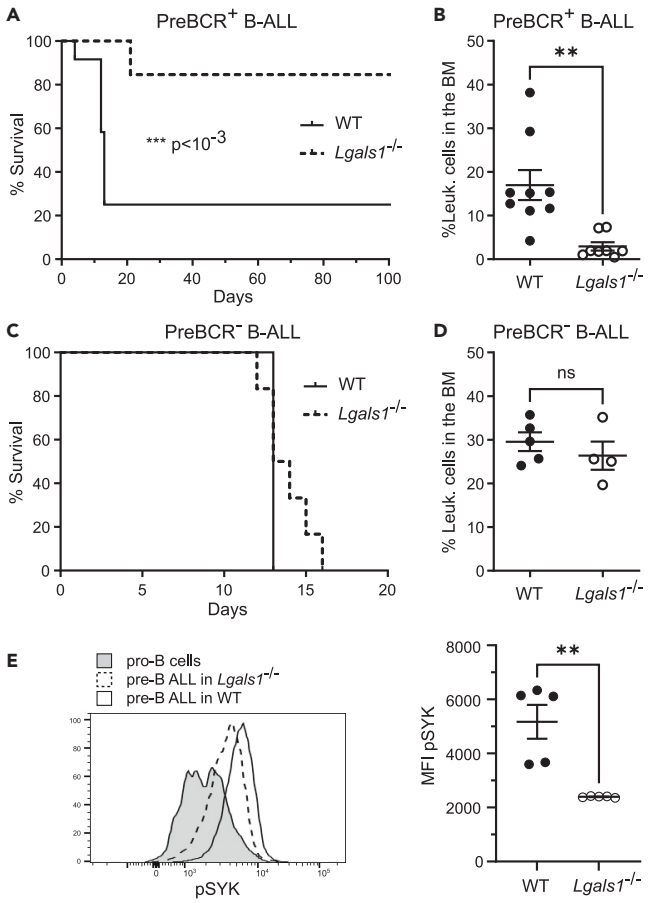

Figure 1. Galectin-1 influences the development of murine Pre-BCR$^+$ B-ALL

(A) Primary pre-B ALL cells from *Blnk*$^{-/-}$*Btk*$^{-/-}$ mice were engrafted into WT (n = 12) or *Lgals1*$^{-/-}$ (n = 13) mice. The survival of the animals was expressed as a Kaplan Meyer survival plot.

(B) The proportion of pre-B ALL cells in the BM was determined by flow cytometry based on CD19, CD71, μH chain, BP1 staining 8 days after injection to WT (n = 9) or *Lgals1*$^{-/-}$ (n = 8). See gating strategy in Figures S1A and 1B.

(C) Primary common B-ALL from transgenic Eμ-Myc mice were injected to WT (n = 6) or *Lgals1*$^{-/-}$ (n = 6) mice. Survival was followed as in (A).

(D) The proportion of common B-ALL cells in the BM was determined 8 days after transplantation to WT (n = 5) or *Lgals1*$^{-/-}$ mice (n = 4) as in (B).

(E) SYK phosphorylation was measured by flow cytometry on *Blnk*$^{-/-}$*Btk*$^{-/-}$ pre-B ALL cells 8 days after transplantation in WT (n = 5) and *Lgals1*$^{-/-}$ mice (n = 5). The phosphorylation level was compared to host CD19$^+$CD117$^+$ pre-BCR$^-$ pro-B cells. A representative histogram is shown in the left panel and mean fluorescence intensity (MFI) from all the samples in the right panel. The MFI of leukemic cells was subtracted from the MFI of the control pro-B cells from the same mouse. Error bars represent SEM. Statistical significance was calculated using unpaired t test with Welsh correction (B) or using Mann-Whitney non-parametric test (E). **p < 0.01; ns: not significant.

Pre-BCR signaling is functional in human pre-B ALL and influences leukemic growth through GAL1-dependent activation

We next determined the influence of GAL1 on human pre-B ALL. GAL1-induced pre-BCR clustering was mimicked using an anti-μ H chain antibody. Although the intensity and duration varied between samples, a calcium flux was induced in the pre-BCR$^+$ Nalm6 cell line and in the pre-B ALL patient samples, indicating that the pre-BCR was functional (Figure 3A). Induction of the calcium flux signal was dependent on activation of the SYK kinase, which is downstream of the pre-BCR, because calcium influx was not detected in the presence of the SYK inhibitor AB8779. Moreover, pre-BCR$^-$ BCR::ABL1$^+$ common B-ALL did not respond to the anti-μH antibody and was insensitive to SYK inhibition. Importantly, pre-BCR signaling is functional regardless of the intrinsic genetic alterations present in the pre-B ALL (Figure 3A and Table S1). Therefore,

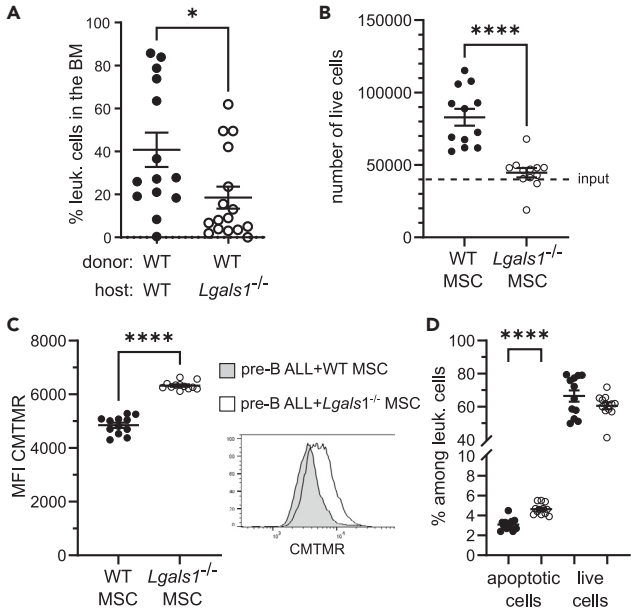

Figure 2. GAL1$^+$ mesenchymal stromal cells favor the development of murine Pre-BCR$^+$ B-ALL

(A) WT (n = 14) and *Lgals1*$^{-/-}$ mice (n = 16) were lethally irradiated and transplanted with WT BM. Following complete hematopoietic reconstitution, the mice were injected with *Blnk*$^{-/-}$*Btk*$^{-/-}$ pre-B ALL cells. The proportion of leukemic cells was determined as in Figure 1B.

(B) *Blnk*$^{-/-}$*Btk*$^{-/-}$ pre-B ALL cells stained with CMTMR were co-cultured with WT or *Lgals1*$^{-/-}$ MSCs during 40 h. The absolute cell number was determined by flow cytometry using Flow-Count Fluorospheres after exclusion of Sytox AAD$^+$ dead cells.

(C) The relative proliferation was determined with the CMTMR MFI (representative histogram on the right panel) and the MFI for all samples is shown in the left panel.

(D) Proportion of apoptotic (Sytox AAD$^-$ Caspase3/7 Green$^+$) and live (Sytox AAD$^-$ Caspase3/7 Green$^-$) leukemic cells in co-culture with WT (black dots) and *Lgals1*$^{-/-}$ (white dots) MSCs. Error bars represent SEM. Statistical significance was calculated using Mann-Whitney non-parametric test (A), or unpaired t test with (C) or without (B and D) Welsh correction. *p < 0.05; ****p < 0.0001.

these results indicate that pre-BCR signaling is functional in human pre-B ALL and is amplified upon pre-BCR clustering.

Pre-B ALL samples were next injected into NOD-SCID-γ_c-deficient (NSG) mice and NSG-*Lgals1*$^{-/-}$ immunodeficient mice. Importantly, pre-BCR/GAL1 interaction occurs across species.[21] E2A::PBX1$^+$ pre-B ALL growth was decreased in *Lgals1*$^{-/-}$ mice (Figures 3B and S2A). As expected, and despite the expression of integrins required for GAL1-dependent pre-BCR signaling (Figure S2B), human pre-BCR$^-$ common B-ALL growth was not affected by the absence of GAL1 (Figure 3C), thus paralleling our observations made with murine B-ALL. Furthermore, these results obtained in an immunodeficient background confirmed that the observed effects were not related to an increased T cell-dependent tumor rejection in absence of GAL1.

We then analyzed SYK and BLNK phosphorylation downstream of the pre-BCR.[4] Phosphorylation was strongly decreased for pre-B ALL in NSG-*Lgals1*$^{-/-}$ mice compared to control mice, with levels close to those observed for pre-BCR$^-$ common B-ALL (Figures 3D and 3E). Furthermore, pre-B ALL proliferation but not survival was decreased in the absence of GAL1 (Figure 3F and S2C), indicating that GAL1-dependent pre-BCR activation sustains pre-B ALL growth.

As pre-BCR cross-linking induces pre-BCR signaling for pre-B ALL samples bearing distinct genetic alterations (Figure 3A), we took advantage of pre-BCR$^+$ BCR::ABL1$^+$ B-ALL cases to challenge our observations. Again, pre-B ALL growth was impaired in the absence of GAL1 (Figures 3G and S2D). Furthermore, SYK and BLNK phosphorylation was significantly decreased in the absence of GAL1, confirming that GAL1 is involved in pre-BCR activation (Figures 3H and 3I). Finally, the growth of pre-BCR$^-$ BCR::ABL1$^+$ common

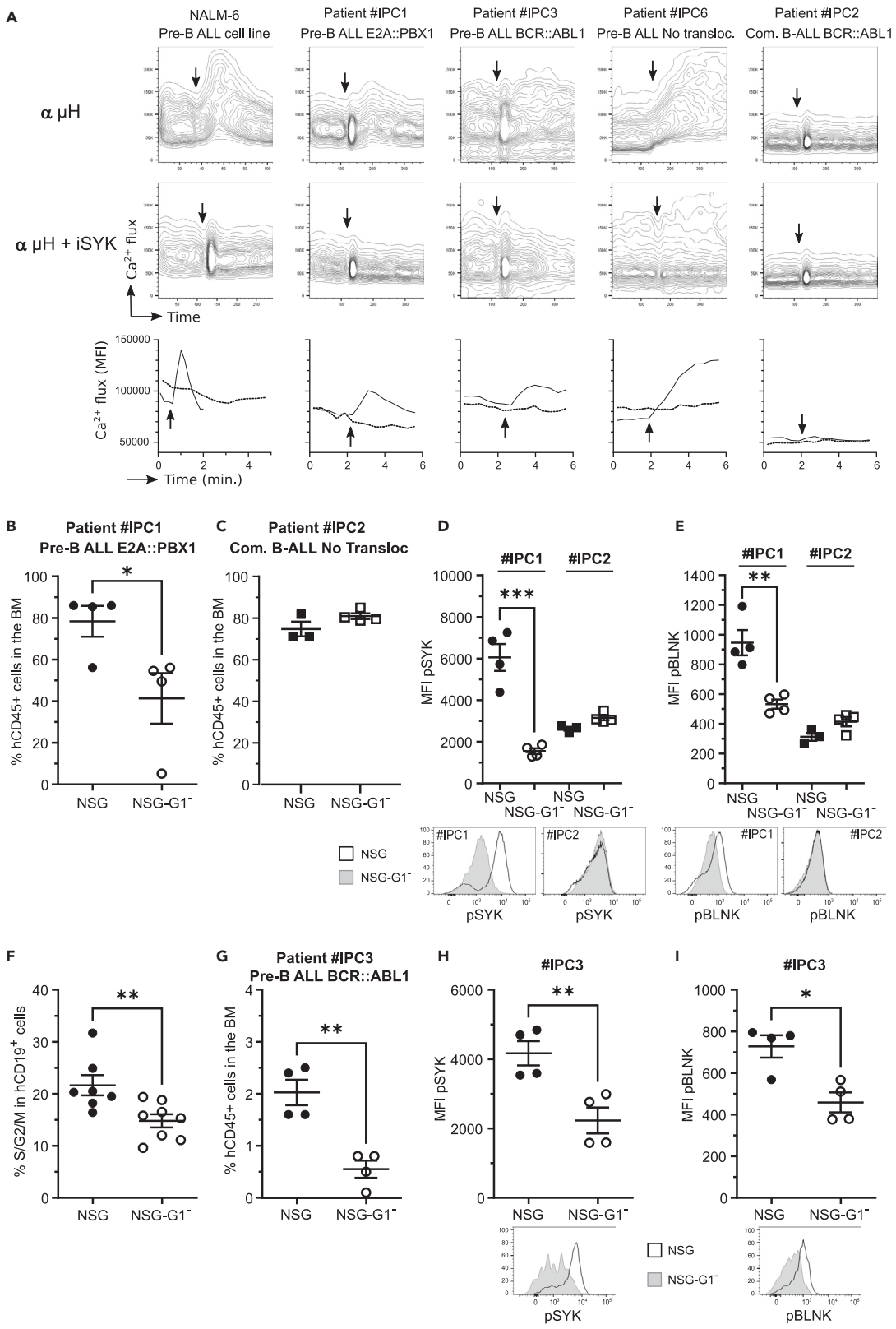
A
NALM-6
Pre-B ALL cell line
Patient #IPC1
Pre-B ALL E2A::PBX1
Patient #IPC3
Pre-B ALL BCR::ABL1
Patient #IPC6
Pre-B ALL No transloc.
Patient #IPC2
Com. B-ALL BCR::ABL1
α μH
α μH + iSYK
Ca2+ flux
Time
Ca2+ flux (MFI)
Time (min.)
B
Patient #IPC1
Pre-B ALL E2A::PBX1
% hCD45+ cells in the BM
NSG
NSG-G1-
C
Patient #IPC2
Com. B-ALL No Transloc
D
#IPC1
#IPC2
MFI pSYK
pSYK
E
MFI pBLNK
pBLNK
F
% S/G2/M in hCD19+ cells
G
Patient #IPC3
Pre-B ALL BCR::ABL1
H
#IPC3
I
#IPC3

Figure 3. Pre-BCR signaling and human pre-B ALL growth are impaired in the absence of GAL1

(A) The pre-BCR$^+$ NALM-6 cell line as well as pre-BCR$^+$ pre-B ALL and pre-BCR$^-$ common B-ALL patient samples were loaded with the PBX calcium indicator. Calcium flux was recorded over time by flow cytometry following stimulation with an anti μH chain antibody in absence or presence of the SYK inhibitor AB8779. The lower panels represent the MFI of the calcium probe over time for the anti μH chain treatment without (continuous line) and with AB8779 (dotted line).

(B) Human pre-B ALL and (C) common B-ALL were xenografted separately to NSG and NSG-*Lgals1*$^{-/-}$ mice. The proportion of CD45$^+$ human leukemic cells in the BM was determined by flow cytometry 10 weeks after transplantation.

The phosphorylation level of SYK (D) and BLNK (E) was determined by flow cytometry for the samples shown in (B) and (C). Representative histograms are shown in the lower panels and MFI from all the samples in the upper panels.

(F) Proportion of human pre-B ALL cells engaged in S/G2/M phases of the cell cycle in the BM of NSG and NSG-*Lgals1*$^{-/-}$ mice.

The proportion of leukemic cells (G) and the phosphorylation of SYK (H) and BLNK (I) were evaluated 10 weeks after transplantation of human BCR::ABL$^+$ pre-B ALL to NSG and NSG-*Lgals1*$^{-/-}$ mice. Statistical significance was calculated using unpaired t test with (D) or without (E,F,G,H) Welsh correction or using Mann-Whitney non-parametric test (B,I). Error bars represent SEM. *p < 0.05; **p < 0.01; ***p < 0.001.

B-ALL was not affected in NSG-*Lgals1*$^{-/-}$ mice (Figure S2E). As GAL1 can be expressed by MLL-rearranged B-ALL and by a small proportion of other subtypes,[22,23] we checked whether the absence of GAL1-dependent growth for common B-ALL was not due to intrinsic GAL1 expression. In opposition to the MLL-rearranged RS4;11 cell line and similarly to the Nalm6 cell line, neither the common B-ALL, nor the pre-B ALL used expressed GAL1 (Figure S2F). Altogether these results, indicate that exogenous GAL1-dependency was specific for pre-B ALL irrespectively of intrinsic genetic alterations.

Pre-B cell receptor clustering and signaling contribute to pre-B acute lymphoblastic leukemia relapse

We next determined whether GAL1-induced pre-BCR clustering could be at the origin of pre-B ALL survival and resistance. Pre-BCR clustering not only involves protein/protein interactions of GAL1 with the pre-BCR, but also interactions of GAL1 with glycosylated chains of integrins.[20] As a consequence, β-galactosides including lactose or thiodigalactoside (TDG) were able to inhibit pre-BCR clustering.[11] We, therefore, determined the capacity of TDG but also OTX008, a calixarene shown to inhibit specifically GAL1 carbohydrate binding, to block GAL1-binding at the surface of pre-B ALL (Nalm6 cell line and sample #IPC6). Surprisingly, in opposition to TDG, which inhibited GAL1-binding in a dose-dependent manner, inhibition by the OTX008 compound was marginal, even at a high toxic dose (Figures S3A and S3B). Furthermore, while OTX008 was also shown to inhibit GAL1 expression in some cancer cell lines,[24] endogenous expression of GAL1 by MSCs was not affected following a 48-h treatment with 10 μM OTX008 (Figure S3C). Based on these results, we chose to evaluate the influence of TDG on pre-B ALL activation and survival. Importantly, Nalm6 co-culture with GAL1$^+$ MSC induced pre-BCR signaling at a similar level as pre-BCR clustering with an anti μH chain antibody and was inhibited by both AB8779 or TDG (Figure S3D).

To study pre-BCR dependent resistance, pre-B ALL blasts were cultivated in low serum (3% instead of 10%) in the presence and in absence of MSCs. In these conditions, Nalm6 cell survival and number were strongly affected by the absence of MSCs as compared to classical culture conditions and were only slightly decreased in presence of MSCs (Figures 4A and 4B). Although the resistance of patient pre-B ALL in starved condition was lower than the Nalm6 immortalized cell line, survival, and cell numbers were increased more than 10- and 5-times respectively in presence of MSCs (Figures 4C and 4D). Most importantly, TDG decreased survival and cell numbers in the presence but not in absence of MSCs. Altogether, these results strongly suggest that GAL1-dependent pre-BCR clustering and activation participate in pre-B ALL survival in their supportive niche.

In order to confirm the contribution of pre-BCR activation to the outgrowth of pre-B ALL *in vivo*, NSG mice were transplanted with BCR::ABL1$^+$ pre-B ALL cells and treated with the BCR:ABL1 inhibitor Nilotinib (Nilo), the BTK inhibitor Ibrutinib (Ibru), or a combination of both. While Nilo had a strong effect on leukemic growth (Figure 4E), Ibru treatment was not sufficient to decrease the tumor burden. It is likely that BCR::ABL1-dependent pathways take over pre-BCR activation as circulating blasts were decreased two weeks after the beginning of the treatment for the combination, as compared to Nilo (Figure 4E). Most importantly, a relapse was observed in the blood 12 days post-Nilo treatment, in contrast to the combination. The latter was clearly beneficial in blood, spleen, and BM compared to untreated controls or each drug alone (Figures 4E–4G). Furthermore, whereas blast numbers were significantly reduced in blood and spleen following Nilo treatment compared to controls, the effect was heterogeneous and not significant in

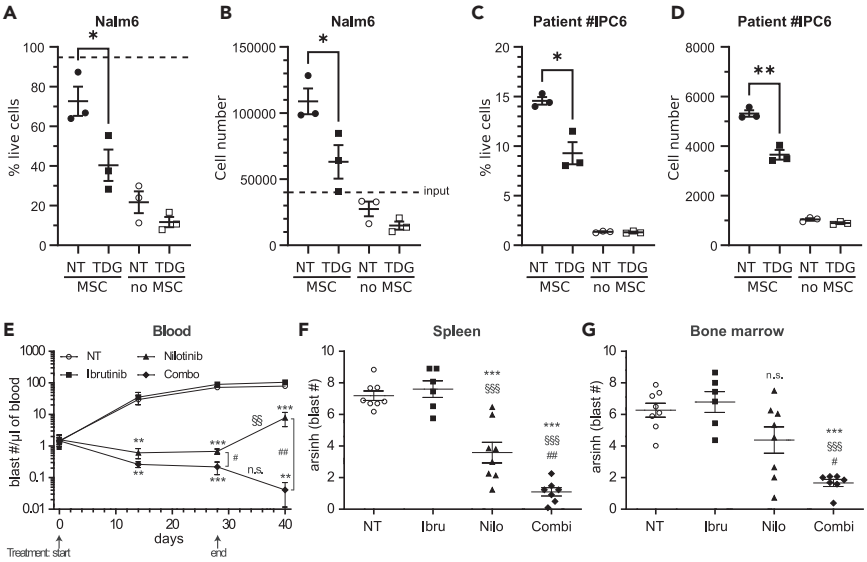

Figure 4. Pre-BCR clustering and signaling contribute to pre-B ALL development in addition to intrinsic oncogenic signals

(A) Nalm6 cells were cultivated during 48 h in low serum (3% serum) in presence or absence of murine WT MSC and treated with thiodigalactoside (TDG) or not (NT). The percentage of Sytox Blue negative live cells is shown. The dotted line represents the proportion of live Nalm6 in normal culture conditions without MSCs (10% serum).

(B) Absolute cell number assessed by flow cytometry using Flow-Count Fluorospheres for Nalm6 cells as shown in (A).

(C) Percentage and (D) absolute number of pre-B ALL from patient #IPC6 cultured as in (A).

(E) BCR::ABL1^{+} pre-B ALL cells from patient #IPC3 were transplanted into NSG mice. When the first human blasts were detected in blood, mice were either not treated (NT) or treated with Ibrutinib, Nilotinib and a combination of both during 4 weeks. The blast number in blood was followed at day 0, 14, 28 and 40. The beginning and the end of treatment are indicated. The statistical significance in (E) has been determined for each time point for non-treated vs. treated animals (*); Nilotinib vs. combination (#); between the last day of treatment and day 12 post-treatment for Nilotinib (§) and combination (n.s.; not significant). Statistical significance was calculated using unpaired t test without Welsh correction (A to E).

(F) In the spleen and (G) in the BM, the blast number was determined 13 days after the end of treatment. Data have been transformed to reach normality and analyzed with an ANOVA with non-treated (*), Ibrutinib-treated (#) and Nilotinib-treated (§) animals as a reference. Error bars represent SEM. *, # or §: $p < 0.05$; **, ##, or §§: $p < 0.01$; ***, ###, or §§§: $p < 0.001$.

the BM. These results show that blocking BCR::ABL1-dependent signaling was effective, but that leukemic escape and relapse occurred in the BM, most likely because of pre-BCR activation.

DISCUSSION

In this study, we report that GAL1 enhances pre-BCR signaling in both murine and human pre-B ALL and sustains leukemic growth. GAL1 binds the pre-BCR through protein-protein interactions and induces normal pre-B cell proliferation and differentiation.[11,25] In accordance with these results, the phosphorylation of tyrosine kinases specifically activated downstream of the pre-BCR is impaired in the absence of GAL1 and in parallel, pre-BCR^{+} leukemic cell proliferation is decreased both *in vivo* and *in vitro*. Importantly, we showed previously that a GAL1-dependent pre-BCR clustering was inducing its activation and pre-B cell proliferation.[11,20] Here we confirm on pre-B ALL patient samples that pre-BCR clustering is indeed required for the induction of efficient signaling (Figure 2A). Furthermore, pre-BCR activation and leukemic cell growth is inhibited by treating pre-B ALL/MSC co-cultures with the β-galactoside TDG.

Apart from its role as a pre-BCR ligand, GAL1 is an s-type lectin that forms a lattice at the cell surface through its specific binding to β-galactosides, and contributes to cancer progression either directly or by repressing the immune response.[26] Following murine leukemic cell injection to immune proficient mice, activated T cells were not increased in absence of GAL1. Furthermore, the tumor burden was specifically decreased for pre-BCR^{+} but not pre-BCR^{-} B-ALL. Finally, decreased proliferation of pre-BCR^{+} pre-B

ALL in absence of GAL1 was also observed in an immunodeficient context for patient-derived xenografts, or for *in vitro* co-cultures with MSCs. Therefore, our results ruled out an increased leukemic cell rejection by the immune system in the absence of GAL1. Among the glycosylated proteins know to interact with GAL1, integrins were expressed by mouse and human leukemic B cells (Figures S1I and S2B). A direct effect of these interactions on leukemic growth is however unlikely as murine and human common B-ALL growth is independent of GAL1. Altogether these data strongly suggest that GAL1 is involved in pre-B ALL growth through pre-BCR activation.

Although a larger cohort would be needed, we found that pre-BCR activation was independent of genetic alterations as observed for five patients with genotypes commonly observed for pre-BCR$^+$ B-ALL, that is patients with E2A::PBX1 or BCR::ABL1 fusion genes a well as with a normal karyotype. Our results obtained with BCR::ABL1 leukemic cells contrast with data showing that the forced expression of a pre-BCR in BCR::ABL1$^+$ B-ALL induces cell-cycle arrest and that pre-BCR signaling component expression has thus to be repressed.[27] In that study, re-expression of BLNK in murine *Blnk*$^{-/-}$ BCR::ABL1-transformed B-ALL and transduction of human BCR::ABL1$^+$ B-ALL with an Igμ chain inhibited leukemic growth. In contrast in another study, BLNK expression levels in humans were found similar between BCR::ABL1$^+$ B-ALL and E2A::PBX1$^+$ pre-B ALL in a large cohort of patients.[18] Furthermore, BLNK and other pre-BCR-associated signaling proteins are phosphorylated in BCR::ABL1$^+$ B-ALL.[19] Finally, both our current results and published findings show that some BCR::ABL1$^+$ B-ALL are pre-BCR-positive.[7] It seems thus likely that pre-BCR$^-$ and pre-BCR$^+$ BCR::ABL1$^+$ B-ALL form distinct subtypes that respond differently to pre-BCR signaling. Re-expression of a pre-BCR in the former has a negative effect on leukemia development, while the latter – similarly to E2A::PBX1$^+$ pre-B ALL – can receive pre-BCR-dependent growth signals following GAL1 interaction.

Our result obtained both *in vivo* and *in vitro* show that pre-BCR activation in pre-B ALL is non-cell-autonomous and depends on the expression of GAL1 by non-hematopoietic cells present in the BM microenvironment. Previous studies have demonstrated the existence of a pre-BCR tonic signal that is ligand-independent and induced by pre-BCR dimerization.[9,28] Accordingly, we observed *ex vivo* a basal calcium flux inhibited with the SYK inhibitor AB8779 for patient #IPC1 and a marginal or undetectable signal for IPC3 and IPC6 respectively (Figure 3A). Interestingly, Erasmus et al. showed that the addition of GAL1 at the surface of pre-B ALL cells induces pre-BCR aggregation and inhibition of pre-BCR signaling.[28] These results are in accordance with our previous work that demonstrated that GAL1 binding at the surface of Nalm6 cells was not sufficient to induce pre-BCR signaling but required in addition clustering at the synapse formed between Nalm6 and MSCs.[21] We now show that inhibition of galectin-dependent pre-BCR clustering with TDG in the presence of MSCs but not in their absence impairs pre-BCR activation and resistance of pre-B ALL in starved condition. Therefore, GAL1 expressed by the pre-B ALL BM cellular niche may favor relapse by sustaining leukemic growth.

Our current and previous studies suggest that inhibiting pre-BCR signaling could be an efficient strategy to limit relapse in complement to classical therapies.[5,6] Indeed, we observed an advantage to combine inhibitors blocking respectively oncogenic (Nilotinib) and pre-BCR signals (Ibrutinib), as compared to blocking only the oncogenic signals. In contrast to a previous study,[6] there was however no effect of Ibrutinib alone. This discrepancy may be due to the fact that, in contrast to our study, Ibrutinib treatment was performed concomitantly with pre-B ALL injection, before leukemic cell seeding in the BM. Indeed, migration in response to CXCL12 or CXCL13 is impaired in *Btk*$^{-/-}$ murine B cells.[29] Furthermore, Ibrutinib inhibits *in vitro* migration of pre-B ALL cells toward CXCL12 and interactions with stromal cells.[6] Altogether these results indicate that pre-BCR activation is accessory to signals transmitted by oncogenic mutations but can have an influence on relapse. The evaluation of the GAL1-specific inhibitor OTX008 was unsuccessful. OTX008 binds GAL1 at the opposite of the carbohydrate recognition domain (CRD) and as a consequence impairs lactose binding.[30] However, in opposition to the β-galactoside TDG, which binds to all the galectin family members, OTX008 was unable to block GAL1 binding to pre-B ALL (Figure S3). One could argue that pre-BCR/GAL1 interaction may hide the binding site of OTX008 and induce resistance to this inhibitor. Alternatively, pre-BCR/GAL1 interaction induces structural changes of the CRD and consequently restricts access to certain β-galactosides at the expense of others.[31] In that context, OTX008 may lose its capacity to inhibit GAL1 binding to particular glycosylated chains, which would be accessible only in presence of the pre-BCR. This hypothesis fits with the fact that OTX008 can inhibit GAL1 binding at the surface of pre-BCR$^-$ B-ALL.[23] The development of new GAL1

inhibitors remains interesting in pre-B ALL treatment as blocking GAL1 with TDG efficiently impaired pre-B ALL growth in co-culture with GAL1-expressing MSCs.

Although the knowledge remains relatively limited, the influence of BM niches on B-ALL resistance to therapy has been observed previously. B-ALL cells in co-culture with MSCs were found to be more resistant to the chemotherapeutic agents cytarabine or etoposide.[32] This protective effect was dependent on adhesive signals mediated by the interaction of the α4β1 integrin at the surface of leukemic cells with its ligand VCAM-1. Thereafter, mice xenografted with B-ALL cells treated with Natalizumab, an anti-α4β1 integrin antibody, in combination with a chemotherapeutic treatment showed an improved survival as compared to mice treated with the chemotherapy alone.[33] In addition, retention of B-ALL in specialized niches of the BM is mediated by the chemokine CXCL12 secreted by MSCs as demonstrated with the transplantation of the Nalm6 cell line or of B-ALL from patients to immunodeficient mice.[34,35] AMD3100 (Plerixafor), antagonist of CXCR4 the CXCL12 receptor, inhibits the homing of leukemic cells to the BM. Furthermore, the treatment of xenografted mice with plerixafor sensitizes B-ALL to cytarabine.[36] Importantly, these molecular cues present in BM niches are primarily known to be involved in the development of normal BM B cells.[8]

In conclusion, our results and those from others clearly show the importance of accessory signals transmitted by the BM microenvironment on leukemic growth, in parallel to cell-autonomous oncogenic signals. Targeting these accessory signals could be beneficial to decrease relapse, in complement to conventional therapies or treatments targeting oncogenic proteins.

Limitations of the study

The current study was performed on a limited number of patient samples. Therefore, it would be important to evaluate the role of pre-BCR/GAL1 binding on pre-B ALL relapse on a larger cohort of patients. Furthermore, although blocking GAL1 with a beta-galactoside was efficient to inhibit pre-B ALL growth *in vitro*, OTX008, the only GAL1 inhibitor available to our knowledge, was inefficient in blocking GAL1 binding to pre-B ALL surface. New GAL1 inhibitors will have to be developed and evaluated *in vivo* for their capacity to decrease pre-B ALL resistance to therapies.

STAR★METHODS

Detailed methods are provided in the online version of this paper and include the following:

- KEY RESOURCES TABLE
- RESOURCE AVAILABILITY
  - Lead contact
  - Materials availability
  - Data and code availability
- EXPERIMENTAL MODEL AND SUBJECT DETAILS
  - Mice and murine primary cells
- METHOD DETAILS
  - Cell culture
  - Treatments
  - Flow cytometry
  - Galectin-1 binding at the cell surface
  - Immunofluorescence imaging
- QUANTIFICATION AND STATISTICAL ANALYSIS

SUPPLEMENTAL INFORMATION

Supplemental information can be found online at https://doi.org/10.1016/j.isci.2023.106385.

ACKNOWLEDGMENTS

We are grateful to the core flow cytometry and the animal facility of the CRCM for providing supportive help, and to Dr. Segolène Duran for providing tyrosine kinase inhibitors. We are also grateful to the ARCHE, flow cytometry, and microscopy core facilities of the UAR Biosit (Rennes) and particularly to Florence Boutillon (ARCHE, UAR Biosit) for technical support.

Financial Support: This work was partly supported by grants from the SIRIC (Inca-Inserm-DGOS 6038), the ARC Foundation (PJA#20131200298 and PJA#20161204555 to S.J.C.M.; PJA#20141201990 to M.A.-L.), the Ligue Nationale Contre le Cancer (#ELN2020), the ADHO association and the Dutch Cancer Society (KWF Grant 2014–6564 to R.W.H.). J.P. was the recipient of PhD grants from the Région PACA/Inserm/Innate Pharma and from La Ligue Nationale contre le Cancer (#TDCU19117), M.B. from FRM (#FDT20150532380) and M.C.D. from la Ligue Nationale contre le Cancer (IP/SC-16060).

AUTHOR CONTRIBUTIONS

J.P and M.B. designed experiments, performed research, and analyzed data; J.D., C.M., M.C.D., T.M., A.-L.B., F.B., E.C., and A.G. performed research and analyzed data; M.J.W.dB., J.R, and C.B. supplied important material and protocols; R.C., Y.C., P.D., K.T., R.W.H, and N.V. discussed data and edited the manuscript. C.S. and M.A.-L. conceptualized research, discussed data, and edited the manuscript; S.J.C.M. conceptualized research, designed experiments, performed research, analyzed data, and wrote the manuscript.

DECLARATION OF INTERESTS

The authors declare no competing financial interests.

INCLUSION AND DIVERSITY

We support inclusive, diverse, and equitable conduct of research.

Received: September 21, 2022
Revised: January 15, 2023
Accepted: March 7, 2023
Published: March 11, 2023

REFERENCES

1. Pui, C.H., Relling, M.V., and Downing, J.R. (2004). Acute lymphoblastic leukemia. N. Engl. J. Med. *350*, 1535–1548. https://doi.org/10.1056/NEJMra023001.

2. Bene, M.C., Castoldi, G., Knapp, W., Ludwig, W.D., Matutes, E., Orfao, A., and van't Veer, M.B. (1995). Proposals for the immunological classification of acute leukemias. European group for the immunological characterization of leukemias (EGIL). Leukemia *9*, 1783–1786.

3. Arber, D.A., Orazi, A., Hasserjian, R.P., Borowitz, M.J., Calvo, K.R., Kvasnicka, H.M., Wang, S.A., Bagg, A., Barbui, T., Branford, S., et al. (2022). International consensus classification of myeloid neoplasms and acute leukemias: integrating morphologic, clinical, and genomic data. Blood *140*, 1200–1228. https://doi.org/10.1182/blood.2022015850.

4. Herzog, S., Reth, M., and Jumaa, H. (2009). Regulation of B-cell proliferation and differentiation by pre-B-cell receptor signalling. Nat. Rev. Immunol. *9*, 195–205. https://doi.org/10.1038/nri2491.

5. Geng, H., Hurtz, C., Lenz, K.B., Chen, Z., Baumjohann, D., Thompson, S., Goloviznina, N.A., Chen, W.Y., Huan, J., LaTocha, D., et al. (2015). Self-enforcing feedback activation between BCL6 and pre-B cell receptor signaling defines a distinct subtype of acute lymphoblastic leukemia. Cancer Cell *27*, 409–425. https://doi.org/10.1016/j.ccell.2015.02.003.

6. Kim, E., Hurtz, C., Koehrer, S., Wang, Z., Balasubramanian, S., Chang, B.Y., Müschen, M., Davis, R.E., and Burger, J.A. (2017). Ibrutinib inhibits pre-BCR(+) B-cell acute lymphoblastic leukemia progression by targeting BTK and BLK. Blood *129*, 1155–1165. https://doi.org/10.1182/blood-2016-06-722900.

7. Jumaa, H., Bossaller, L., Portugal, K., Storch, B., Lotz, M., Flemming, A., Schrappe, M., Postila, V., Riikonen, P., Pelkonen, J., et al. (2003). Deficiency of the adaptor SLP-65 in pre-B-cell acute lymphoblastic leukaemia. Nature *423*, 452–456. https://doi.org/10.1038/nature01608.

8. Delahaye, M.C., Salem, K.I., Pelletier, J., Aurrand-Lions, M., and Mancini, S.J.C. (2020). Toward therapeutic targeting of bone marrow leukemic niche protective signals in B-cell acute lymphoblastic leukemia. Front. Oncol. *10*, 606540. https://doi.org/10.3389/fonc.2020.606540.

9. Ubelhart, R., Bach, M.P., Eschbach, C., Wossning, T., Reth, M., and Jumaa, H. (2010). N-linked glycosylation selectively regulates autonomous precursor BCR function. Nat. Immunol. *11*, 759–765. https://doi.org/10.1038/ni.1903.

10. Mourcin, F., Breton, C., Tellier, J., Narang, P., Chasson, L., Jorquera, A., Coles, M., Schiff, C., and Mancini, S.J.C. (2011). Galectin-1-expressing stromal cells constitute a specific niche for pre-BII cell development in mouse bone marrow. Blood *117*, 6552–6561. https://doi.org/10.1182/blood-2010-12-323113.

11. Espeli, M., Mancini, S.J.C., Breton, C., Poirier, F., and Schiff, C. (2009). Impaired B-cell development at the pre-BII-cell stage in galectin-1-deficient mice due to inefficient pre-BII/stromal cell interactions. Blood *113*, 5878–5886. https://doi.org/10.1182/blood-2009-01-198465.

12. Kersseboom, R., Middendorp, S., Dingjan, G.M., Dahlenborg, K., Reth, M., Jumaa, H., and Hendriks, R.W. (2003). Bruton's tyrosine kinase cooperates with the B cell linker protein SLP-65 as a tumor suppressor in Pre-B cells. J. Exp. Med. *198*, 91–98. https://doi.org/10.1084/jem.20030615.

13. Jamrog, L., Chemin, G., Fregona, V., Coster, L., Pasquet, M., Oudinet, C., Rouquié, N., Prade, N., Lagarde, S., Cresson, C., et al. (2018). PAX5-ELN oncoprotein promotes multistep B-cell acute lymphoblastic leukemia in mice. Proc. Natl. Acad. Sci. USA *115*, 10357–10362. https://doi.org/10.1073/pnas.1721678115.

14. Perillo, N.L., Pace, K.E., Seilhamer, J.J., and Baum, L.G. (1995). Apoptosis of T cells mediated by galectin-1. Nature *378*, 736–739. https://doi.org/10.1038/378736a0.

15. Liu, S.D., Tomassian, T., Bruhn, K.W., Miller, J.F., Poirier, F., and Miceli, M.C. (2009). Galectin-1 tunes TCR binding and signal transduction to regulate CD8 burst size. J. Immunol. *182*, 5283–5295. https://doi.org/10.4049/jimmunol.0803811.

16. Rubinstein, N., Alvarez, M., Zwirner, N.W., Toscano, M.A., Ilarregui, J.M., Bravo, A.,

Mordoh, J., Fainboim, L., Podhajcer, O.L., and Rabinovich, G.A. (2004). Targeted inhibition of galectin-1 gene expression in tumor cells results in heightened T cell-mediated rejection; a potential mechanism of tumor-immune privilege. Cancer Cell *5*, 241–251. https://doi.org/10.1016/s1535-6108(04)00024-8.

17. Lee, R.D., Munro, S.A., Knutson, T.P., LaRue, R.S., Heltemes-Harris, L.M., and Farrar, M.A. (2021). Single-cell analysis identifies dynamic gene expression networks that govern B cell development and transformation. Nat. Commun. *12*, 6843. https://doi.org/10.1038/s41467-021-27232-5.

18. Imai, C., Ross, M.E., Reid, G., Coustan-Smith, E., Schultz, K.R., Pui, C.H., Downing, J.R., and Campana, D. (2004). Expression of the adaptor protein BLNK/SLP-65 in childhood acute lymphoblastic leukemia. Leukemia *18*, 922–925. https://doi.org/10.1038/sj.leu.2403349.

19. Chen, Z., Shojaee, S., Buchner, M., Geng, H., Lee, J.W., Klemm, L., Titz, B., Graeber, T.G., Park, E., Tan, Y.X., et al. (2015). Signalling thresholds and negative B-cell selection in acute lymphoblastic leukaemia. Nature *521*, 357–361. https://doi.org/10.1038/nature14231.

20. Rossi, B., Espeli, M., Schiff, C., and Gauthier, L. (2006). Clustering of pre-B cell integrins induces galectin-1-dependent pre-B cell receptor relocalization and activation. J. Immunol. *177*, 796–803.

21. Gauthier, L., Rossi, B., Roux, F., Termine, E., and Schiff, C. (2002). Galectin-1 is a stromal cell ligand of the pre-B cell receptor (BCR) implicated in synapse formation between pre-B and stromal cells and in pre-BCR triggering. Proc. Natl. Acad. Sci. USA *99*, 13014–13019. https://doi.org/10.1073/pnas.202323999.

22. Juszczynski, P., Rodig, S.J., Ouyang, J., O'Donnell, E., Takeyama, K., Mlynarski, W., Mycko, K., Szczepanski, T., Gaworczyk, A., Krivtsov, A., et al. (2010). MLL-rearranged B lymphoblastic leukemias selectively express the immunoregulatory carbohydrate-binding protein galectin-1. Clin. Cancer Res. *16*, 2122–2130. https://doi.org/10.1158/1078-0432.CCR-09-2765.

23. Paz, H., Joo, E.J., Chou, C.H., Fei, F., Mayo, K.H., Abdel-Azim, H., Ghazarian, H., Groffen, J., and Heisterkamp, N. (2018). Treatment of B-cell precursor acute lymphoblastic leukemia with the Galectin-1 inhibitor PTX008. J. Exp. Clin. Cancer Res. *37*, 67. https://doi.org/10.1186/s13046-018-0721-7.

24. Astorgues-Xerri, L., Riveiro, M.E., Tijeras-Raballand, A., Serova, M., Rabinovich, G.A., Bieche, I., Vidaud, M., de Gramont, A., Martinet, M., Cvitkovic, E., et al. (2014). OTX008, a selective small-molecule inhibitor of galectin-1, downregulates cancer cell proliferation, invasion and tumour angiogenesis. Eur. J. Cancer *50*, 2463–2477. https://doi.org/10.1016/j.ejca.2014.06.015.

25. Elantak, L., Espeli, M., Boned, A., Bornet, O., Bonzi, J., Gauthier, L., Feracci, M., Roche, P., Guerlesquin, F., and Schiff, C. (2012). Structural basis for galectin-1-dependent pre-B cell receptor (pre-BCR) activation. J. Biol. Chem. *287*, 44703–44713. https://doi.org/10.1074/jbc.M112.395152.

26. Girotti, M.R., Salatino, M., Dalotto-Moreno, T., and Rabinovich, G.A. (2020). Sweetening the hallmarks of cancer: Galectins as multifunctional mediators of tumor progression. J. Exp. Med. *217*, e20182041. https://doi.org/10.1084/jem.20182041.

27. Trageser, D., Iacobucci, I., Nahar, R., Duy, C., von Levetzow, G., Klemm, L., Park, E., Schuh, W., Gruber, T., Herzog, S., et al. (2009). Pre-B cell receptor-mediated cell cycle arrest in Philadelphia chromosome-positive acute lymphoblastic leukemia requires IKAROS function. J. Exp. Med. *206*, 1739–1753. https://doi.org/10.1084/jem.20090004.

28. Erasmus, M.F., Matlawska-Wasowska, K., Kinjyo, I., Mahajan, A., Winter, S.S., Xu, L., Horowitz, M., Lidke, D.S., and Wilson, B.S. (2016). Dynamic pre-BCR homodimers fine-tune autonomous survival signals in B cell precursor acute lymphoblastic leukemia. Sci. Signal. *9*, ra116. https://doi.org/10.1126/scisignal.aaf3949.

29. de Gorter, D.J.J., Beuling, E.A., Kersseboom, R., Middendorp, S., van Gils, J.M., Hendriks, R.W., Pals, S.T., and Spaargaren, M. (2007). Bruton's tyrosine kinase and phospholipase Cgamma2 mediate chemokine-controlled B cell migration and homing. Immunity *26*, 93–104. https://doi.org/10.1016/j.immuni.2006.11.012.

30. Dings, R.P.M., Miller, M.C., Nesmelova, I., Astorgues-Xerri, L., Kumar, N., Serova, M., Chen, X., Raymond, E., Hoye, T.R., and Mayo, K.H. (2012). Antitumor agent calixarene 0118 targets human galectin-1 as an allosteric inhibitor of carbohydrate binding. J. Med. Chem. *55*, 5121–5129. https://doi.org/10.1021/jm300014q.

31. Bonzi, J., Bornet, O., Betzi, S., Kasper, B.T., Mahal, L.K., Mancini, S.J., Schiff, C., Sebban-Kreuzer, C., Guerlesquin, F., and Elantak, L. (2015). Pre-B cell receptor binding to galectin-1 modifies galectin-1/carbohydrate affinity to modulate specific galectin-1/glycan lattice interactions. Nat. Commun. *6*, 6194. https://doi.org/10.1038/ncomms7194.

32. Mudry, R.E., Fortney, J.E., York, T., Hall, B.M., and Gibson, L.F. (2000). Stromal cells regulate survival of B-lineage leukemic cells during chemotherapy. Blood *96*, 1926–1932.

33. Hsieh, Y.T., Gang, E.J., Geng, H., Park, E., Huantes, S., Chudziak, D., Dauber, K., Schaefer, P., Scharman, C., Shimada, H., et al. (2013). Integrin alpha4 blockade sensitizes drug resistant pre-B acute lymphoblastic leukemia to chemotherapy. Blood *121*, 1814–1818. https://doi.org/10.1182/blood-2012-01-406272.

34. Sipkins, D.A., Wei, X., Wu, J.W., Runnels, J.M., Côté, D., Means, T.K., Luster, A.D., Scadden, D.T., and Lin, C.P. (2005). In vivo imaging of specialized bone marrow endothelial microdomains for tumour engraftment. Nature *435*, 969–973. https://doi.org/10.1038/nature03703.

35. Juarez, J., Dela Pena, A., Baraz, R., Hewson, J., Khoo, M., Cisterne, A., Fricker, S., Fujii, N., Bradstock, K.F., and Bendall, L.J. (2007). CXCR4 antagonists mobilize childhood acute lymphoblastic leukemia cells into the peripheral blood and inhibit engraftment. Leukemia *21*, 1249–1257. https://doi.org/10.1038/sj.leu.2404684.

36. Sison, E.A.R., Magoon, D., Li, L., Annesley, C.E., Rau, R.E., Small, D., and Brown, P. (2014). Plerixafor as a chemosensitizing agent in pediatric acute lymphoblastic leukemia: efficacy and potential mechanisms of resistance to CXCR4 inhibition. Oncotarget *5*, 8947–8958. https://doi.org/10.18632/oncotarget.2407.

37. Poirier, F., and Robertson, E.J. (1993). Normal development of mice carrying a null mutation in the gene encoding the L14 S-type lectin. Development *119*, 1229–1236. https://doi.org/10.1242/dev.119.4.1229.

38. Ta, V.B.T., de Bruijn, M.J.W., ter Brugge, P.J., van Hamburg, J.P., Diepstraten, H.J.A., van Loo, P.F., Kersseboom, R., and Hendriks, R.W. (2010). Malignant transformation of Slp65-deficient pre-B cells involves disruption of the Arf-Mdm2-p53 tumor suppressor pathway. Blood *115*, 1385–1393. https://doi.org/10.1182/blood-2009-05-222166.

39. Harris, A.W., Pinkert, C.A., Crawford, M., Langdon, W.Y., Brinster, R.L., and Adams, J.M. (1988). The E mu-myc transgenic mouse. A model for high-incidence spontaneous lymphoma and leukemia of early B cells. J. Exp. Med. *167*, 353–371. https://doi.org/10.1084/jem.167.2.353.

40. Dexter, T.M., Allen, T.D., and Lajtha, L.G. (1977). Conditions controlling the proliferation of haemopoietic stem cells in vitro. J. Cell. Physiol. *91*, 335–344. https://doi.org/10.1002/jcp.1040910303.

41. Rip, J., de Bruijn, M.J.W., Kaptein, A., Hendriks, R.W., and Corneth, O.B.J. (2020). Phosphoflow protocol for signaling studies in human and murine B cell subpopulations. J. Immunol. *204*, 2852–2863. https://doi.org/10.4049/jimmunol.1901117.

42. Salles, A., Billaudeau, C., Sergé, A., Bernard, A.M., Phélipot, M.C., Bertaux, N., Fallet, M., Grenot, P., Marguet, D., He, H.T., and Hamon, Y. (2013). Barcoding T cell calcium response diversity with methods for automated and accurate analysis of cell signals (MAAACS). PLoS Comput. Biol. *9*, e1003245. https://doi.org/10.1371/journal.pcbi.1003245.

43. Kawamoto, T., and Shimizu, M. (2000). A method for preparing 2- to 50-micron-thick fresh-frozen sections of large samples and undecalcified hard tissues. Histochem. Cell Biol. *113*, 331–339. https://doi.org/10.1007/s004180000149.

STAR★METHODS

KEY RESOURCES TABLE

REAGENT or RESOURCE	SOURCE	IDENTIFIER
Antibodies		
Mouse CD2 PE-Cy7 Clone RM2-5	Biolegend	Cat#100114, RRID: AB_2563092
Mouse CD4 PE-CF594 Clone RM4-5	BD Biosciences	Cat#562285, RRID: AB_11154410
Mouse CD8a PerCP-Cy5.5 Clone 53-6.7	BD Biosciences	Cat#561109, RRID: AB_394081
Mouse CD19 PE-Cy5.5 Clone 1D3	eBioscience	Cat#35-0193-82, RRID: AB_891395
Mouse CD31 BUV395 Clone MEC13.3	BD Biosciences	Cat#740231, RRID: AB_2739979
Mouse CD44 APC-Cy7 Clone IM7	BD Biosciences	Cat#560568, RRID: AB_1727481
Mouse CD45 BUV395 Clone 30-F11	BD Biosciences	Cat#564279, RRID: AB_2651134
Mouse CD45 PE-Cy5.5 Clone 30-F11	eBioscience	Cat#35-0451-82, RRID: AB_469718
Mouse CD45 Alexa Fluor 700 Clone 30-F11	BD Biosciences	Cat#560510, RRID: AB_1645208
Mouse CD45 APC-eFluor 780 Clone 30-F11	eBioscience	Cat#47-0451-82, RRID: AB_1548781
Mouse CD45R/B220 APC-eFluor 780 Clone RA3-6B2	eBioscience	Cat#47-0452-82, RRID: AB_1518810
Mouse CD45.1 APC Clone A20	eBioscience	Cat# 17-0453-82, RRID: AB_469398
Mouse CD49d PE Clone R1-2	eBioscience	Cat#25-0492-82, RRID: AB_2811776
Mouse CD49e/CD29 PE Clone eBioHMa5-1	eBioscience	Cat#11-0493-81, RRID: AB_1234968
Mouse CD51 BV650 Clone RMV-7	BD Biosciences	Cat#740546, RRID: AB_2870640
Mouse CD71 BV605 Clone C2	BD Biosciences	Cat#563013, RRID: AB_2737950
Mouse CD106 BUV496 Clone 429	BD Biosciences	Cat#752532, none
Mouse CD249 Biotin Clone 6C3	BD Biosciences	Cat#553159, RRID: AB_394671
Mouse β7 integrin PE Clone M293	BD Biosciences	Cat#557498, RRID: AB_396735
Mouse Endomucin purified Clone V.7C7	Santa Cruz	Cat#sc-65495, RRID: AB_2100037
Mouse Galectin-1 purified Clone 201002	R&D Systems	Cat#MAB12451, RRID: AB_2136636
Mouse Igκ BV421 Clone 187.1	BD Biosciences	Cat#562888, RRID: AB_2737867
Mouse Igλ BV421 Clone R26-46	BD Biosciences	Cat#744523, RRID: AB_2742297
Mouse μH chain BV421 Clone R6-60.2	BD Biosciences	Cat#562595, RRID: AB_2737671
Mouse μH chain Alexa-Fluor 488 Goat Polyclonal	Southern Biotech	Cat#1021-30, RRID: AB_2794251
Mouse μH chain PE Goat Polyclonal	Southern Biotech	Cat#1021-09, RRID: AB_2794244
Mouse Sca-1 BUV737 Clone D7	BD Biosciences	Cat#749199, RRID: AB_2873577
Human CD10 PE-Cy5 Clone HI10α	BD Biosciences	Cat#561676, RRID: AB_395777
Human CD19 PE-CF594 Clone HIB19	BD Biosciences	Cat#562321, RRID: AB_11154408
Human CD19 PE-Cy7 Clone HIB19	BD Biosciences	Cat#560728, RRID: AB_1727438
Human CD45 Pacific Blue Clone HI30	Biolegend	Cat#304022, RRID: AB_493655
Human CD45 FITC Clone J33	Beckman Coulter	Cat#IM0782U, RRID: AB_131000
Human CD45 BV711 Clone HI30	BD Biosciences	Cat#564357, RRID: AB_2744404
Human CD49d PE Clone 9F10	BD Biosciences	Cat#555503, RRID: AB_395893
Human CD49e BV421 Clone IIA1	BD Biosciences	Cat#740077, RRID: AB_2739840
Human β7 integrin APC Clone FIB504	BD Biosciences	Cat#551082, RRID: AB_398490
Human H chain PE Clone G20-127	BD Biosciences	Cat#555783, RRID: AB_396118
Human μH chain purified Goat Polyclonal	ThermoFisher	Cat# A18837, RRID: AB_2535614
Human Galectin-1 purified	R&D Systems	Cat#AF1152, RRID: AB_2136626
Mouse/Human Syk pY348 PE Clone I120-722	BD Biosciences	Cat#558529, RRID: AB_647247
Mouse/Human Blnk pY84 PE Clone J117-1278	BD Biosciences	Cat#558442, RRID: AB_647182

(*Continued on next page*)

Continued

REAGENT or RESOURCE	SOURCE	IDENTIFIER
Rat IgG (H + L) Alexa-Fluor 488 Donkey polyclonal	Jackson Immunoresearch	Cat#712-545-153, RRID: AB_2340684
Goat F(ab')2 IgG (H + L) Alexa -Fluor 647 Donkey polyclonal	Jackson Immunoresearch	Cat#115-606-003, RRID: AB_2338921
Streptavidin PE-CF594	BD Biosciences	Cat#562318, RRID: AB_11154598
Biological samples		
Patient-derived xenografts (PDX)	This paper	N/A
Primary murine leukemic cells from *Blnk*$^{-/-}$*Btk*$^{-/-}$ mice	Ta et al., 2010	N/A
Primary murine leukemic cells from PAX5-ELN mice	This paper	N/A
Primary murine leukemic cells from Eμ-Myc mice	Dr JE Ricci Laboratory	N/A
Primary mesenchymal stromal cells from C57Bl/6J mice	This paper	N/A
Primary mesenchymal stromal cells from *Lgals1*$^{-/-}$ mice	This paper	N/A
Chemicals, peptides, and recombinant proteins		
Sytox Blue	ThermoFisher	Cat#S11348
LIVE/DEAD Fixable Aqua Dead Cell Stain	ThermoFisher	Cat#L34965
LIVE/DEAD Fixable Far Red Cell Stain	ThermoFisher	Cat#L10120
DRAQ7	Beckman Coulter	Cat# B25595
7-AAD	ThermoFisher	Cat#A1310
Nilotinib	Novartis	N/A
Ibrutinib	Janssen Inc.	N/A
AB8779	AB Science	N/A
OTX008	MedChemExpress	Cat#HY-19756
Thiodigalactoside	MedChemExpress	Cat#HY-130208
Critical commercial assays		
CellTracker™ Orange CMTMR Dye	ThermoFisher	Cat#C2927
Alexa Fluor 488 Antibody Labeling Kit	ThermoFisher	Cat#A20181
CellEvent™ Caspase-3/7 Green Detection Reagent	ThermoFisher	Cat#C10423
Countbright absolute counting beads	ThermoFisher	Cat#C36950
Flow-Count Fluorospheres	Beckman Coulter	Cat#7547053
PBX Calcium assay kit	BD Biosciences	Cat#640176
Dead Cell Removal Kit	Miltenyi Biotec	Cat#130-090-101
BD Cytofix/Cytoperm	BD Biosciences	Cat#554714, RRID: AB_2869008
PerFix EXPOSE	Beckman Coulter	Cat#B26967
SCEM embedding medium	Section-Lab	N/A
Experimental models: Cell lines		
Nalm6	Cellausorus	CVCL_0092
RS4; 11	Cellausorus	CVCL_0093
Experimental models: Organisms/strains		
Mouse: C57Bl/6JRj	Janvier Labs	C57Bl/6JRj
Mouse: Ly5.1	Charles River	B6.SJL-Ptprc^{a}Pepc^{b}/BoyCrl
Mouse: NSG	Charles River	NOD.Cg-Prkdc^{scid} Il2rg^{tm1Wjl}/SzJ
Mouse: *Lgals1*$^{-/-}$	Poirier and Robertson, 1993	N/A
Software and algorithms		
DiVa version 9	BD Biosciences	http://www.bdbiosciences.com/
FlowJo version 10.8	BD Biosicences	https://www.flowjo.com/
Fiji version 1.53	ImageJ	https://fiji.sc/
GraphPad Prism version 9.5.0	GraphPad	https://www.graphpad.com/

RESOURCE AVAILABILITY

Lead contact

Further information and requests for resources and reagents should be directed to and will be fulfilled by the lead contact, Stéphane J.C. Mancini (stephane.mancini@univ-rennes.fr).

Materials availability

This study did not generate new unique reagents. The data generated in this study are available within the article and its supplemental data files.

Data and code availability

- Microscopy data reported in this paper will be shared by the lead contact upon request.
- This study did not generate any code.
- Any additional information required to reanalyze the data reported in this paper is available from the lead contact upon request.

EXPERIMENTAL MODEL AND SUBJECT DETAILS

Mice and murine primary cells

Lgals1$^{-/-}$ mice[37] were backcrossed for more than 8 generations onto the C57Bl/6J and NOD/Scid/*Il2rg*$^{-/-}$ (NSG) background. 6- to 12-week-old mice of both sexes were randomly included and distributed equally in experimental groups. Mice were housed under specific pathogen-free conditions in the animal facility of the CRCM and of the UAR Biosit. For the generation of BM chimeras, WT or *Lgals1*$^{-/-}$ recipient mice were lethally irradiated at 7 Gy with an X-ray source (RS-200 irradiator) one day before reconstitution with 5x10^6 Ly5.1-C57Bl/6J bone marrow by intra-venous injection. Leukemic cells were injected after full reconstitution of the hematopoietic system. Mice were handled in accordance with the French Guidelines for animal handling (Agreement #02294.01 and #C35-238-40) and the EU Directive 2010/63/EU.

Primary pre-BCR$^+$ Pre-B ALL isolated from *Blnk*$^{-/-}$*Btk*$^{-/-}$ mice and Pax5-Eln (P5E) transgenic mice of C57Bl/6 background[12,13,38] were maintained in culture in IMDM or RPMI respectively, supplemented with 10% FCS, 5 mM β-Mercaptoethanol, 100 U/ml penicillin, 100 µg/mL streptomycin and murine IL7. Primary pre-BCR$^-$ common B-ALL isolated from transgenic Eμ-Myc mice[39] (kind gift from Dr JE Richie) were cultivated in DMEM 10% FCS 100 U/ml penicillin, 100 µg/mL streptomycin. 5x10^6 *Blnk*$^{-/-}$*Btk*$^{-/-}$ pre-B ALL cells were injected to WT and *Lgals1*$^{-/-}$ animals. Mice were sacrificed one week after injection, before the appearance of symptoms, for flow cytometry analyses, or at the appearance of symptoms following a limit point submitted to the ethical committee, to determine the overall survival. The same procedure was performed with 2.5x10^5 P5E pre-B ALL cells and 5 x10^5 Eμ-Myc common B-ALL cells.

MSCs were prepared from WT and *Lgals1*$^{-/-}$ total bone marrow cells as described previously.[40] Briefly, bone marrow cells were cultured in MEM$_\alpha$, 10% FCS, 100 U/ml penicillin, 100 µg/mL streptomycin at 37 °C, 5% CO2. After the complete loss of non-adherent cells and the establishment of a layer of adherent cells, cells were passed and maintained in MEM$_\alpha$ 20% FCS. The phenotype of MSC was confirmed by the expression of CD51 and Sca-1 and the absence of the hematopoietic and endothelial markers CD45 and CD31 respectively. The expression of GAL1 was controlled with an anti mouse GAL1 antibody (R&D Systems) conjugated with the Alexa-Fluor 488 antibody labeling kit (Thermo Fisher).Patient samples and human cell lines.

The pre-BCR$^+$ Nalm6 and the pre-BCR$^-$ RS4; 11 cell lines were cultivated in RPMI 10% FCS, 100 U/ml penicillin, 100 µg/mL streptomycin. Human common B-ALL (intracellular Igμ$^-$) and pre-B ALL (intracellular Igμ$^+$/IgL$^-$) samples (Table S1) were obtained after informed consent in line with the Declaration of Helsinki and stored in the IPC/CRCM tumor bank. The study protocol was approved by the institutional review board at Institut Paoli-Calmettes (Agreement #15-003). Samples were first xenografted to NSG mice sub-lethally irradiated at 1.5 Gy of total body irradiation. Mice were transplanted with 0.5 to 1x10^6 donor cells one day after irradiation by intra-venous injection via the retro-orbital sinus. Engraftment was monitored by following human CD45 cells in blood every 2 weeks until mice reached the limit point. Bone marrow cells were then frozen to obtain a biobank of the different samples used in the study. Samples were then thawed and 20'000 leukemic cells were transplanted simultaneously to NSG and NSG-*Lgals1*$^{-/-}$ mice sub-lethally

irradiated at 1.5 Gy. Mice were sacrificed whenever the proportion of hCD45$^+$ cells reached about 50% in the blood as a maximum and the blast load in the BM was determined by flow cytometry.

METHOD DETAILS

Cell culture

Blnk$^{-/-}$*Btk*$^{-/-}$ pre-B ALL cells were stained with 4 μM CMTMR Orange (ThermoFisher) during 20 min at 37 °C. Dead cells were removed using the Dead Cell Removal kit (Miltenyi Biotec). Cells were then co-cultured with WT or *Lgals1*$^{-/-}$ MSCs in RPMI 10% FCS, 5 mM β-Mercaptoethanol, 100 U/ml penicillin, 100 μg/mL streptomycin, without IL7 in 24-well plates during 40 h at 37 °C, 5% CO2. Cells were then flushed and washed in cold PBS before their analysis by flow cytometry.

Leukemic cells from patient #IPC6 (Table S1), from which dead cells were removed using the Dead Cell Removal kit, and Nalm6 cells were cultivated in presence or in absence of murine WT MSCs in RPMI with 5% or 3% FCS respectively in 24-well plates during 40 h at 37 °C, 5% CO2. Cells were cultivated in presence or in absence of 1 mM thiodigalactoside. Cells were then flushed and washed in cold PBS before their analysis by flow cytometry. Dead cells were stained with Sytox Blue and the absolute cell count was obtained using Flow-Count Fluorospheres (Beckman Coulter).

Treatments

NSG mice were xenografted with a BCR:ABL1$^+$ pre-B ALL sample (patient #IPC3, see Table S1). After the first hCD45$^+$ blasts were detected in the blood, four groups were formed and mice were immediately treated by gavage 5 days a week the first week and 4 days a week the next 3 weeks as follows: Control (PEG400/10% DMSO), Nilotinib (60 mg/kg the first week, 30 mg/kg thereafter), Ibrutinib (30 mg/kg) and Nilotinib/Ibrutinib combination. Blast number was monitored at day zero, day 14, day 28 of treatment and at day 12 post treatment. Mice were sacrificed one day after the last bleeding. Absolute counts were determined by flow cytometry using the Countbright absolute counting beads (ThermoFisher).

Flow cytometry

Femurs and tibias were flushed with FACS Buffer (PBS 1X, 0.1% FSC, 2 mM EDTA). Red blood cells were lysed (Gibco ACK Lysing Buffer) and mouse or human leukemic B cells stained with antibodies 20 min at 4 °C. Dead cells were excluded using Sytox Blue, LIVE/DEAD Fixable Aqua Dead Cell Stain (Thermo Fisher), LIVE/DEAD Fixable Far Red Cell Stain (Thermo Fisher) or DRAQ7 (Beckman Coulter). Intracellular stainings were performed using the BD Cytofix/Cytoperm Fixation/Permeablization kit (BD Biosciences). The analysis of phosphorylated proteins was performed as described previously[41] by using the anti-phosphoprotein antibodies pSYK and pBLNK with the PerFix EXPOSE Kit (Beckman Coulter) following the manufacturer instructions. At least 500 events were recorded in the leukemic cell gate.

Pre-BCR activation of Nalm6 in co-culture with murine WT MSC was performed as follow. Nalm6 were starved 90 min in RPMI 0.2% FCS and next incubated 90 min in presence or in absence of murine WT MSCs without treatment, with 1 μM of the SYK tyrosine kinase inhibitor AB8779 (kind gift from AB Science) or with 1 mM thiodigalactoside (MedChemExpress). As a control of pre-BCR activation, Nalm6 cells were incubated 15 min with 10 μg/mL goat anti human μH chain (Thermo Fisher) alone or together with 1 μM AB8779. pBLNK staining was performed using the PerFix EXPOSE Kit.

Cell cycle analysis was performed with 7-AAD following cellular permeabilization with the BD Cytofix/Cytoperm Fixation/Permeablization Kit (BD Biosciences). Apoptosis was analyzed with the CellEvent™ Caspase-3/7 Green Detection Reagent (ThermoFisher).

Calcium flux initiated after pre-BCR clustering was measured using the PBX Calcium Assay Kit (BD Biosciences) as described previously.[42] Briefly, cells were loaded with the calcium indicator in 0.1% FCS 1h at 37 °C, 5% CO2. Cells were acquired on the flow cytometer for approximately 2 min at 37 °C before the addition of 10 μg/mL goat anti human μH chain (Thermo Fisher) alone or together with 1 μM of the SYK tyrosine kinase inhibitor AB8779 (kind gift from AB Science). The acquisition was then maintained during 4–5 min.

FACS analysis was performed on a LSRII SORP or a Fortessa X20 (BD Biosciences). Data were analyzed using DiVa Version 9 (BD Biosciences) or FlowJo Version 10 (TreeStar) softwares.

Galectin-1 binding at the cell surface

Pre-B ALL from patient #IPC6 and Nalm6 were incubated 30 min at 4 °C in PBS with 70 nM recombinant human GAL1 (kind gift from Dr. L. Elantak) in absence or in presence of different concentrations of thiodigalactoside or of the GAL1 inhibitor OTX008 (MedChemExpress). Cells were then stained with a purified goat anti hGAL1 antibody (R&D Biosystems) followed by an Alexa-Fluor 647 F(ab')2 donkey anti goat IgG (H + L) (Jackson ImmunoResearch) and analyzed by flow cytometry.

Immunofluorescence imaging

Blnk$^{-/-}$*Btk*$^{-/-}$ pre-B ALL cells were stained with 4 μM CMTMR Orange (ThermoFisher) during 20 min at 37 °C. Dead cells were removed using the Dead Cell Removal kit (Miltenyi Biotec). WT and *Lgals1*$^{-/-}$ mice were sacrificed 1 day after i.v. injection of CMTMR^{+} cells. For frozen sections of long bones, femurs were fixed in 4% paraformaldehyde (PFA) overnight at 4 °C. For cryopreservation, the bones were incubated sequentially in 10%, 20%, and 30% sucrose/PBS at 4 °C for 1h each, embedded and flash frozen in SCEM embedding medium (SECTION-LAB). Frozen sections were prepared 20 μm thick with a Cryostat (CM3050, Leica) using Kawamoto's tape transfer method.[43] Sections were stained with a rat anti-endomucin antibody (Santa Cruz) followed by an Alexa-Fluor 488-conjugated donkey anti-rat IgG secondary antibody (Jackson ImmunoResearch). Slides were then mounted with Mowiol (Merck) antifade reagent supplemented with Sytox Blue nucleic acid stain (Thermo Fisher) and analyzed by confocal microscopy on a SP5 (Leica Microsystems). ImageJ software (National Institutes of Health) was used for image analysis.

QUANTIFICATION AND STATISTICAL ANALYSIS

The number of biological replicates is indicated in figure legends. Error bars for pooled replicates represent standard error of the mean (SEM). The distribution of samples was determined by applying the D'Agostino-Pearson normality test for experiments with more than 12 samples and the Shapiro-Wilk normality test for smaller numbers. Samples were compared with a two-tailed unpaired t test when normality was reached and a Welsh correction was applied whenever the variance between samples was different. When normality was not reached, the analysis was performed with a Mann-Whitney non-parametric test. Comparison of multiple samples was performed with the one-way analysis of variance (ANOVA) statistical model. Transformation has been performed when necessary to reach normality and has been stated in the concerned figures. p values: *$p < 0.05$; **$p < 0.01$; ***$p < 0.001$; ****$p < 0.00001$. All statistical analyses were performed with GraphPad Prism 9.